Enabling Body-Centric Computing Applications with LED-to-Camera Communication

Omer Dalgic
University of Applied Sciences and Arts of Southern Switzerland (SUPSI)
Lugano, Switzerland
omer.dalgic@supsi.ch

Daniele Puccinelli
University of Applied Sciences and Arts of Southern Switzerland (SUPSI)
Lugano, Switzerland
daniele.puccinelli@supsi.ch

Marco Zúñiga
Delft University of Technology (TU Delft)
Delft, The Netherlands
m.a.zunigazamalloa@tudelft.nl

ABSTRACT

Advances in Visible Light Communication are enabling novel Internet of Things applications. Going forward, we expect that LED-to-Camera links will enable a wide range of body-centric computing applications. Up until now, most LED-to-Camera studies have been following a deploy-and-test approach instead of a principled methodology. This ad-hoc design raises up two problems. First, we cannot compare fairly the various methods proposed in the literature because they use different types of LEDs and cameras. Second, and perhaps more importantly, we cannot identify the fundamental opportunities and limits of these novel links. To overcome these challenges, we propose a simple analytical model that estimates the range and data rate of LED-to-camera links prior to deployment. The model is built from first principles and requires only a limited set of parameters. To validate the accuracy of our model, we consider the two main transmission modes used in the literature: binary transmission and communication based on the rolling shutter effect. Our experimental evaluation confirms the predictions of the analytical model.

CCS Concepts

• **Computing methodologies** → **Modeling and simulation**; • **Human-centered computing** → **Human computer interaction (HCI)**.

Keywords

visible light communication, camera, analytical model

ACM Reference Format:

Omer Dalgic, Daniele Puccinelli, and Marco Zúñiga. 2022. Enabling Body-Centric Computing Applications with LED-to-Camera Communication. In *ACM Workshop on Body-Centric Computing Systems (BodySys'22), July 1, 2022, Portland, OR, USA.* ACM, New York, NY, USA, 6 pages. https://doi.org/10.1145/3539489.3539588

1 INTRODUCTION

Nowadays, thanks to advances in Visible Light Communication (VLC), the intensity of LEDs can be modulated to transmit information without causing any flickering effect. The impact of VLC on the Internet of Things (IoT) is already noticeable because almost all light sources in our environments are based on LEDs. Given the ubiquity of smartphones, we anticipate that LED-to-Camera VLC links will also have a far-reaching impact as an enabling technology for body-centric computing applications.

The pervasive presence of LED-to-Camera links is enabling a wide range of novel applications, in particular for the area of Human-Computer Interaction (HCI). HCI is gaining prominence as the number of smart embedded devices continues to increase [1] and is paving the way to a host of applications that can greatly benefit from LED-to-Camera communication. Smartphone cameras have already played a central role in various body-centric HCI applications, primarily as a sensing device [2, 3]. We believe that LED-to-Camera communication can pave to way to more body-centric applications where the camera serves as a communication device between humans and the infrastructure that surrounds them.

Our key contribution is a simple analytical model for LED-to-Camera communication. We also build a system prototype to validate the model and carry out link evaluation.

2 BACKGROUND

In LED-to-Camera (L2C) links, the smartphone camera receives information by detecting the intensity of the light source in each frame. Over the past few years, there has been a great deal of interest in this type of link. Examples include Augmented Reality, indoor localization, and smart-city applications [4–11].

L2C communication can employ binary or rolling shutter transmission (Figure 1). With binary transmission, one frame corresponds to a single bit of information and the light source is completely ON or OFF in the frame. Therefore, the data rate is constrained by the camera frame rate. Nowadays, most smartphones provide between 30 and 240 frames per second (fps), which limits the data rate of binary transmissions to a few tens or a few hundred bits-per-second (bps).

The limitations of binary transmission can be overcome by exploiting the rolling shutter effect, which leverages an image capture method available with most CMOS (camera) sensors. The rolling shutter effect allows the transmission of multiple bits per frame because, instead of capturing the entire image at once, the image is captured row-by-row. In a CMOS sensor, the time required to capture a single frame (t_f) depends on two key parameters: the exposure time (t_e) and the readout time (t_r). The t_e parameter determines the amount of time each row remains open to collect light (i.e. sense the image), and the t_r parameter determines the amount of time needed to read the pixel values for each row [12] (i.e. store the image).

If a single bit duration is greater than a frame duration, all the pixels covered by the light source are perceived as either completely ON or completely OFF (binary transmission, Figure 1a). Instead, if the light intensity changes faster than the frame period, different rows will observe different light intensities, resulting in a zebra pattern where each band corresponds to an individual bit (rolling shutter transmission, Figure 1b). For the example presented in Figure 1, the rolling shutter transmission conveys five bits per frame.

Figure 2 describes in more detail how the image is generated on smartphones. The duration of the exposure time is the same

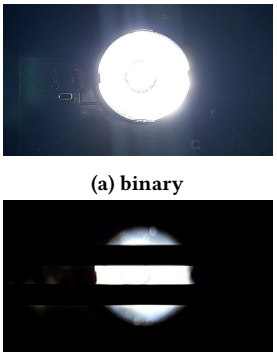

(a) binary

(b) rolling shutter

Figure 1: two types of transmission: Binary and RS.

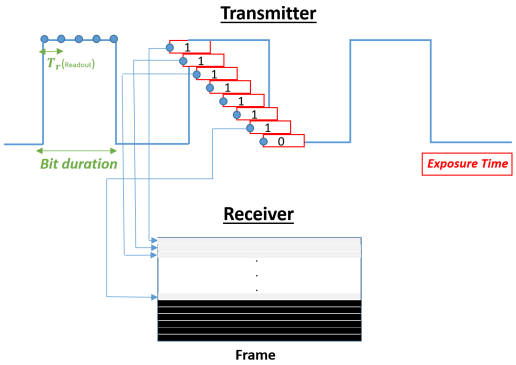

Figure 2: the appearance of the frame on the smartphone is based on various parameters from the transmitter and the receiver.

for each row, but the start of the exposure time changes because it is delayed by the readout time. For each row, the collected light is converted into gray-scale values that are proportional to the amount of received light: 255 for white, 0 for black. For example, for the square wave generated by the LED we have the following outcomes. If the exposure time is completely covered by the ON (OFF) period, we get a sensor value of 255 (0), but the boundaries between bits show gray rows because they cover periods with and without incoming light.

To ensure reliable communication with rolling shutter transmission, a single bit duration must be longer than the exposure time of the camera. Otherwise, all rows would obtain a shade of gray, making it harder to distinguish ones and zeros. In addition to that, the size of the light source (captured within the image) must be large enough to capture multiple rows, else, binary transmission is the only option.

3 ANALYTICAL MODEL

In this section, we illustrate a simple analytical model for L2C communication that serves to estimate the range and capacity of LED-to-camera links. The model assumes that a single LED is transmitting to a single smartphone screen using basic OOK. The input parameters are the smartphone model, the phone screen orientation (portrait or landscape), the LED diameter, the OOK bit rate, and the distance between the transmitting LED and the receiving smartphone (the LED is assumed to be facing the screen with a clear line of sight). The type of smartphone determines all the basic camera properties such as resolution, focal length, frame rate, length of one pixel in the sensor. The camera resolution determines the total number of pixels per frame. The diameter of the transmitter LED provides information about the total number of pixels that represent the transmitter LED in a received frame. The OOK bit rate determines the single bit duration. Finally, the distance between the transmitter LED and the smartphone impacts the size of the LED on the received frame. For a specific link between an LED and a smartphone camera, the model determines the geometric size of the light source (as a pixel count) and infers the transmission type (binary transmission or rolling shutter). This is used to predict the appearance of the received frames and determines the data rate and achievable range.

The bit rate is the product of the total number of bits from a single frame (number of bands) and the frame rate of the camera. In binary transmission, the achievable data rate is equal to the frame rate of the camera. In rolling shutter transmission, the achievable data rate mostly depends on the number of pixels that represent the transmitter LED in the received frames.

The RS mechanism has the advantage of receiving multiple bits from a single image thanks to the presence of multiple bands. Each of these bands corresponds to a single bit of information, and the total number of bands in a frame determines the number of bits of information that can be transmitted through the frame. In the case of the rolling shutter, the number of bits in the single frame mainly depends on two parameters: the total number of pixels for the light source on the image sensor and the width of the band in the frame.

Equation 1 indicates the total number of pixels for the light source when the camera takes pictures [13]. The focal length of the camera (f_0) and the length of one pixel (S_p) depend on camera type.

$$S_{ip} = \frac{S_0 f_0}{(D_0 - f_0) S_p} \tag{1}$$

- S_{ip} = Size of the LED (In terms of number of pixels)
- S_0 = Diameter of the LED (mm)
- f_0 = Focal length of the camera (mm)
- D_0 = Distance between camera and LED (mm)
- S_p = Length of one pixel in the sensor (mm)

The total number of pixels must be calculated in video mode for L2C communication. At a given distance, objects in video mode look larger than in picture mode. Figure 3, shows the difference between an image taken in picture mode (left) and one taken in video mode (right), with the photographed object at the same distance from the camera in both images. The video coefficient (c_v) is added into Equation 1 as a multiplication factor to obtain the size of the light source in video mode (Equation 2).

Moreover, the resolution of the video mode and picture mode is different from each other in smartphones. For this reason, the number of pixels for the light source must be scaled into video resolutions from the photo resolutions (N_v and N_p are smaller resolution values based on portrait and landscape orientations. For

Figure 3: picture mode (left) versus video mode (right) at the same distance from the camera.

the portrait orientation, the frame width is considered in terms of the number of pixels. For the landscape orientation, the frame height is taken). S_v is the number of pixels for the light source in the case of the video mode.

$$S_v = \frac{S_0 f_0 c_v}{(D_0 - f_0) S_p} \frac{N_v}{N_p} \tag{2}$$

The frame duration can be computed as $t_f = t_e + N t_r + t_i$, where N is the total number of rows for the landscape orientation of the phone, and t_e is the exposure time. The single-frame duration depends on the fps of the smartphone camera, and this duration is inversely proportional to the fps. There is a time gap between two consecutive frames, and it is called the inter-frame duration (t_i). The frame duration also covers the inter-frame duration. The camera readout time (t_r) is obtained based on the value of the exposure time, frame duration, and inter-frame duration. In addition to the size of the light source, the width of the band is another critical factor for the data rate. The width of the band depends on the readout time and the modulation frequency (f). It is determined by calculating the amount of the readout time for a single bit as $W_b = \frac{1}{t_r f}$.

The average number of bits in a single frame can be computed by dividing the total number of pixels for a light source by the width of the bands. The width of the band is nearly constant for most bands (it may vary by one or two pixels). However, the width of the first or the last band in the frame may be smaller then the width of the other bands. This happens because the LED may not cover the entire frame, causing a loss of information from the first/last band. The first/last band may also be formed by residual pixels; in such cases, we have a residual band contributing and extra bit of information. Therefore, the total number of bands may vary in different frames. Finally, the OOK bit rate is obtained as the product of the frame rate and the number of bits in a single frame as

$$N_s = \frac{S_v + W_b - 1}{W_b} \tag{3}$$

4 EXPERIMENTAL VALIDATION

To carry out an experimental validation of our model, we build a simple prototype of an LED transmitter to smartphone camera pair. Our transmitter uses a MCE4WT LED on an Arduino-UNO board with OOK modulation. Our receiver is a Galaxy-A7 smartphone running the Open Camera application, which enables us to adjust the exposure time. The recorded video is broken into frames that are processed with a standard image processing pipeline based on OpenCv[1]. Synthetic frames and experimentally collected frames are compared in terms of the width of the bands, the LED size, and the frame appearance for rolling shutter transmission, and in terms of the LED size and the frame appearance for binary transmission.

[1]https://opencv.org/

Parameters/Values			
Phone Model	Galaxy A7	Frame duration	24.24 ms
LED Size	2.06 cm	Inter frame duration	9.09 ms
Modulation Frequency	1 kHz	Video Resolution	(1080, 1920)
Duty Cycle	46%	Photo Resolution	(4248, 5664)
Distance	15 cm	Pixel Length	$0.9\mu m$
Data Sequence	[1,0,0,1,1,1, 0,1,0,1,1,0,0]	Exposure Time	1/71429 s
Focal Length	3.93 mm	Video Coefficient	1.33

Table 1: parameters used in the experiment.

Table 1 shows the parameters and their values for the experiments. The duration of the ON time is longer than the duration of the OFF time when the duty cycle is 50% due to the fall and rise times of the LED. The duty cycle of the LED is adjusted as 46% to have an equal duration for zeros and ones. Moreover, the same data sequence is sent repeatedly. The modulation frequency is controlled with custom software running on the Arduino board. The distance and the exposure time of the camera are constant during recording.

The LED size and the width of the bands are obtained based on the number of pixels in the frame by means of image processing. Each frame is converted into a gray-scale format in order to have a single-pixel value proportional to the light intensity. Moreover, the image is blurred with a Gaussian function to reduce the noise, and thresholding is applied to obtain a binary image. Finally, the white parts of the image are filtered to detect the light source, so that we can measure the size of the LED, the width of the bands, and the data rate.

The analytical model enables us to estimate the size of the LED and the width of the bands. The model can also generate three consecutive synthetic frames based on the input parameters provided by the user. Synthetic frames are helpful for a visual comparison of the model output to experimental results. The input parameters identify the information required in Figure 2 (bit duration, readout time, and number of the pixel representing the light source). The OOK bit rate determines the LED waveform and single bit duration (the LED waveform is generated based on the desired data sequence in the experiment). The readout time (t_r) depends on the smartphone model. The LED diameter, the smartphone model, and the distance provide information related to the number of pixels for the light source (S_v).

Figure 4 compares three consecutive experimental and synthetic frames. The total size of the LED in the experiment varies between 212 and 217 pixels, slightly more than the 209 pixels expected based on our model from Equation 2. The width of the bands for a single bit is predicted to be 45 pixels by our model and varies between 44 and 46 pixels for a single bit in our experimental results.

Figure 5 shows sample waveforms for three frames based on pixel values along the vertical diameter of the light source. Because

(a) first frame

(b) second frame

(c) third frame

Figure 4: sample frames in the RS scenario (distance = 15 cm).

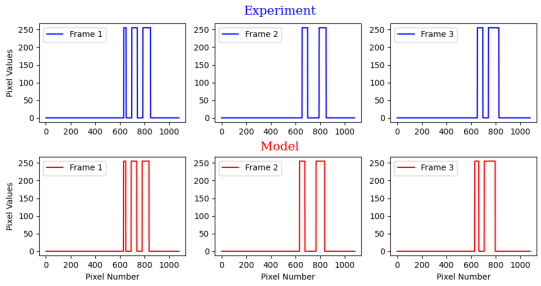

Figure 5: pixel values along the vertical diameter of the light source (RS).

(a) appearances of the first frame

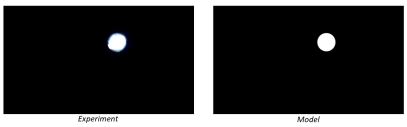

(b) appearances of the second frame

(c) appearances of the third frame

Figure 6: comparison of the model and the experiment images for binary transmission (distance = 17 cm).

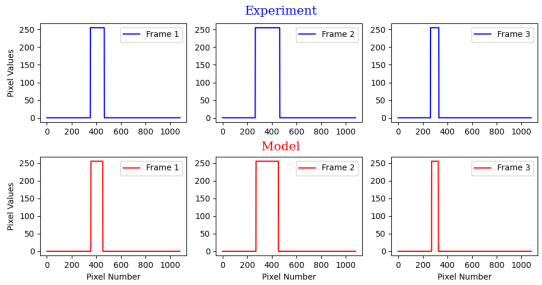

Figure 7: pixel values along the vertical diameter of the light source (binary transmission).

of the binary filter, the waveform oscillates between values of 0 and 255 pixels. The experimental waveforms are considerably close to the synthetic waveforms from the model. Possible deviations may be introduced by the fluctuation of the frame rate and the inter-frame duration of the camera as well as the difference of the total pixel count for the light source between synthetic and experimental frames.

Experiments are carried out when the bit duration is 66 ms which corresponds to two frames duration for Galaxy A7. A bit sequence of {1,0} is transmitted. The distance between pairs is 17 cm. The exposure time of the camera is 1/71429 s. Three consecutive frames are shown for the experimentally generated frames and synthetically generated frames (Figure 6). In the experiment, the diameter of the circle covers 195-199 pixels. In the model, it is 184 pixels (Equation 2). Moreover, waveforms have close values for zero and one bits in terms of the number of pixels (Figure 7).

5 EVALUATION

The analytical model evaluates the effect of the transmitter-receiver distance on the size of the LED in the camera frame and on the data rate. In this section, analytical results are compared with real-world experiments.

The distance between the LED and the smartphone screen has a significant impact on rolling shutter transmission, while it affects binary transmission to a lesser extent. The size of the LED on the frame gets smaller as the LED moves away from the smartphone, thus challenging rolling shutter transmission when the width of the band becomes comparable to the size of the LED on the frame, because the width of the band does not depend on the transmitter-receiver distance in rolling shutter transmission. Therefore, determining the LED size on the frame is critical for L2C communication. The size of the LED in the camera frame helps determine up to which point rolling shutter transmission is viable for a given transmitter-receiver pair. The size of the LED also determines the data rate, especially for rolling shutter transmission (Equation 3).

The simple prototype from Section 4 is used to carry out experiments for the measurement of the size of the LED and the data rate over a range of transmitter-receiver distances in order to validate the accuracy of the analytical model. The experiments are conducted with a transmitter-receiver distance ranging from 10 cm to 60 cm using a Samsung Galaxy A7 smartphone.

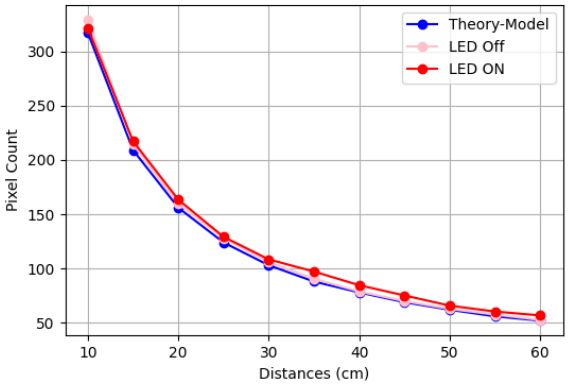

Figure 8: pixel count for the LED transmitter for distances between 10 and 60 cm.

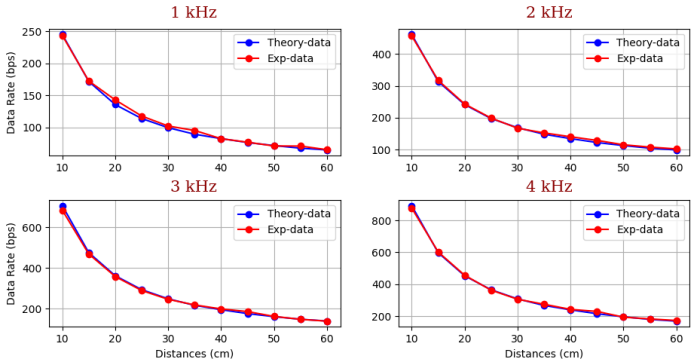

Figure 9: data rate for different modulation frequencies for the Galaxy A7 smartphone.

Equation 2 provides the size of the object in the frame in terms of the number of pixels. For the light source, the diameter of the LED is taken into account. However, light sources may have a halo effect, which causes the enlargement of the object on the frame in the experiments. Practically, the diameter of the object becomes larger due to the presence of extra brightness around the circle-shape lens. For this reason, the total number of pixels for the LED is measured both when the LED is off and when it is on. In the experiments, we only consider the pixel count for the circle-shape lens in the frame when the LED is off. In the analytical results, the pixel count for the LED remains constant independently of the LED state; in the experiments, however, the pixel count changes due to the halo effect.

In Figure 8, the number of pixels representing the LED in the camera frame (both as predicted by the model and as measured in our experiments) is shown as a function of transmitter-receiver distance. We carried out measurements at transmitter-receiver distances ranging between 10 and 60 cm at 5 cm intervals (the reported pixel count for each distance is averaged over five measurements). The experimental results confirm the analytical results in terms of pixel count for the LED when the the LED is off. When the LED is on, due to the halo effect, we observe a relatively minor mismatch between the analytical results and the experimental results.

In Figure 9, the data rate values for different modulation frequencies are shown for the Galaxy A7 smartphone; we juxtapose our analytical results (from Equation 3) to our experimental results for a transmitter-receiver distance ranging from 10 cm to 60 cm. The bit rate reported at each distance is the average over five experiments. We minimize the halo effect by arranging the orientation of the LED with respect to the smartphone camera. We note that the analytical model ignores the halo effect and therefore determines the minimum data rate for a specific link. We observe a relatively minor deviation between the experimental results and the analytical results.

6 RELATED WORK

In our work, we analyze the performance of the L2C communication. Since the appearance of the frames determines the possible range and the data rate in L2C links, synthetic frames are created based on our analytical model. There are several examples of previous work that analyzes the performance of L2C links [14], [15] and synthetic frame creation [16].

In [16], the authors create synthetic frames for Color Multiplexed OOK modulation by benefiting from the radiation pattern of an LED and camera optics. They do not provide any analytical evaluation of the performance of L2C links. In [14], the authors provide a performance evaluation of L2C communication with a redundancy mechanisms (packet repetition). Specifically, they study the probability of failing to receive a packet when the packet is repeated several times.

In [15], the authors analyze the maximum data rate and signal to interference plus noise ratio of L2C links. However, they do not validate their model through experimental verification with real smartphone cameras. Moreover, they make overly simplified assumptions, such as assuming a zero inter-frame gap time.

7 CONCLUSION

Given the ubiquity of smartphones and LEDs, L2C communication can potentially be very beneficial to body-centric computing applications. In this work, we have introduced an analytical model for L2C communication that serves to determine the frame appearance and the data rate for a specific L2C link. The analytical model is validated through real-world experiments. Three consecutive frames from the experiment and the model are compared to evaluate the reliability of the model. The width of the bands and size of the light source have close values in terms of the number of pixels for two categories of the frames. The analytical model helps to control the communication properties (data rate, range, etc.) for the given pair of the LED and the smartphone before their usage in real-time.

Acknowledgement

The authors gratefully acknowledge the financial support of the European Commission, provided through the European Training Network in Low-Energy Visible Light IoT Systems (ENLIGHT'EM) under grant agreement H2020-MSCA-ITN-2018 nº 814215.

References

[1] G. J. Kim, Human-computer interaction: fundamentals and practice. CRC press, 2015.

[2] M. M. Gharasuie, N. Jennings, and S. Jain, "Performance monitoring for exercise movements using mobile cameras," in Proceedings of the Workshop on Body-Centric Computing Systems, BodySys'21, (New York, NY, USA), p. 1–6, Association for Computing Machinery, 2021.

[3] D. Kim, K. Park, and G. Lee, OddEyeCam: A Sensing Technique for Body-Centric Peephole Interaction Using WFoV RGB and NFoV Depth Cameras, p. 85–97. New York, NY, USA: Association for Computing Machinery, 2020.

[4] K. Ahuja, S. Pareddy, R. Xiao, M. Goel, and C. Harrison, "Lightanchors: Appropriating point lights for spatially-anchored augmented reality interfaces," in Proceedings of the 32nd Annual ACM Symposium on User Interface Software and Technology, pp. 189–196, 2019.

[5] J. Yang and J. A. Landay, "Infoled: Augmenting led indicator lights for device positioning and communication," in Proceedings of the 32nd Annual ACM Symposium on User Interface Software and Technology, pp. 175–187, 2019.

[6] Z. Yang, Z. Wang, J. Zhang, C. Huang, and Q. Zhang, "Wearables can afford: Light-weight indoor positioning with visible light," in Proceedings of the 13th Annual International Conference on Mobile Systems, Applications, and Services, pp. 317–330, 2015.

[7] Y. Yang, J. Hao, and J. Luo, "Ceilingtalk: Lightweight indoor broadcast through led-camera communication," IEEE Transactions on Mobile Computing, vol. 16, no. 12, pp. 3308–3319, 2017.

[8] H.-Y. Lee, H.-M. Lin, Y.-L. Wei, H.-I. Wu, H.-M. Tsai, and K. C.-J. Lin, "Rollinglight: Enabling line-of-sight light-to-camera communications," in Proceedings of the 13th Annual International Conference on Mobile Systems, Applications, and Services, pp. 167–180, 2015.

[9] P. Ji, H.-M. Tsai, C. Wang, and F. Liu, "Vehicular visible light communications with led taillight and rolling shutter camera," in 2014 IEEE 79th Vehicular Technology Conference (VTC Spring), pp. 1–6, IEEE, 2014.

[10] Y. Yang, J. Nie, and J. Luo, "Reflexcode: Coding with superposed reflection light for led-camera communication," in Proceedings of the 23rd Annual International Conference on Mobile Computing and Networking, pp. 193–205, 2017.

[11] R. Boubezari, H. Le Minh, Z. Ghassemlooy, and A. Bouridane, "Smartphone camera based visible light communication," Journal of Lightwave Technology, vol. 34, no. 17, pp. 4121–4127, 2016.

[12] C. Danakis, M. Afgani, G. Povey, I. Underwood, and H. Haas, "Using a cmos camera sensor for visible light communication," in 2012 IEEE Globecom Workshops, pp. 1244–1248, IEEE, 2012.

[13] S. Verma, "Analysing the Performance and Stability of LED-to-Camera Links," Master's thesis, Delft University of Technology, the Netherlands, 2017.

[14] A. Duque, R. Stanica, A. Desportes, and H. Rivano, "Performance evaluation of led-to-camera communications," in Proceedings of the 22nd International ACM Conference on Modeling, Analysis and Simulation of Wireless and Mobile Systems, pp. 135–142, 2019.

[15] T.-H. Do and M. Yoo, "Performance analysis of visible light communication using cmos sensors," Sensors, vol. 16, no. 3, p. 309, 2016.

[16] V. Matus, V. Guerra, C. Jurado-Verdu, J. Rabadán, and R. Perez-Jimenez, "Simulation of rolling shutter acquisition in optical camera communications," in 2019 15th International Conference on Telecommunications (ConTEL), pp. 1–5, IEEE, 2019.